Set-based state estimation for discrete-time constrained nonlinear systems: An approach based on constrained zonotopes and DC programming[☆]

Alesi A. de Paula[a,*], Davide M. Raimondo[b], Guilherme V. Raffo[a,c], Bruno O.S. Teixeira[a,c]

[a] *Graduate Program in Electrical Engineering, Universidade Federal de Minas Gerais, Belo Horizonte, MG, Brazil*
[b] *Department of Electrical, Computer and Biomedical Engineering, University of Pavia, Italy*
[c] *Department of Electronic Engineering, Universidade Federal de Minas Gerais, Belo Horizonte, MG, Brazil*

ARTICLE INFO

Keywords:
Constrained zonotopes
Set-membership filtering
Discrete-time nonlinear systems
DC programming
Nonlinear invariants
Linear inequality constraints

ABSTRACT

This paper introduces a novel state estimator designed for discrete-time nonlinear dynamical systems that encompass unknown-but-bounded uncertainties, along with state linear inequality and nonlinear equality constraints. Our algorithm is based on constrained zonotopes (CZs) and employs a DC programming approach (where DC stands for difference of convex functions). Recently, techniques such as mean value extension and first-order Taylor extension have been adapted from zonotopes to facilitate the propagation of CZs across nonlinear mappings. While the resulting algorithms, known as CZMV and CZFO, achieve higher precision compared to the original zonotopic versions, they still exhibit sensitivity to the wrapping and dependency effects inherent in interval arithmetic. These interval-related challenges can be mitigated through the use of DC programming, as it allows for the determination of approximation error bounds by solving optimization problems. One direct advantage of this technique is the elimination of the dependency effect. Our set-membership filter, referred to as CZDC, provides an alternative solution to CZMV and CZFO. To showcase the effectiveness of our proposed approach, we conducted experiments using CZDC on two numerical examples.

1. Introduction

Set-based techniques have been explored in the literature for addressing a range of problems, including parameter estimation (Bravo, Alamo, & Camacho, 2006a; Bravo, Alamo, Redondo, & Camacho, 2008), state estimation (de Paula, Raffo, & Teixeira, 2022; Rego, Scott, Raimondo, & Raffo, 2021), fault diagnosis (Hast, Findeisen, & Streif, 2015; Xu, Puig, Ocampo-Martinez, Olaru, & Stoican, 2015), control design (Bravo, Alamo, & Camacho, 2006b; Mesbah, 2016), among others. In these instances, sets are employed to represent unknown-but-bounded uncertainties. The effectiveness of set-based techniques has been demonstrated through their application in various domains, including fault detection and isolation in industrial application (Hast et al., 2015), fault diagnosis for wind turbines (Tabatabaeipour, Odgaard, Bak, & Stoustrup, 2012), dynamic robot localization and mapping (Di Marco, Garulli, Giannitrapani, & Vicino, 2004), active localization of stationary features using range-only sensors for mobile robots (Grocholsky, Stump, & Kumar, 2006), vehicle state estimation (Ifqir, Puig, Ichalal, Ait-Oufroukh, & Mammar, 2020), and robot-assisted dressing (Li, Stouraitis, Gienger, Vijayakumar, & Shah, 2021).

Set-based filtering can be categorized into two branches: interval observers and set-membership observers (Pourasghar, Puig, & Ocampo-Martinez, 2019). In this context, our focus is on the latter, where a key distinction lies in the incorporation of intersections among sets to merge forecast and measurement sets. Recently, constrained zonotopes (CZs) have motivated new advancements in set-membership techniques, primarily due to their ability to efficiently represent any convex polytope. The class of CZs expands the zonotopes (centrally symmetric convex polytopes) by incorporating linear equality constraints. One immediate benefit of this extension is the ability to propagate asymmetric polytopes while retaining the computational advantages of zonotopes. Additionally, by introducing a generalized intersection operation among CZs that can be computed exactly, it becomes possible, in principle, to eliminate the loss of precision compared to zonotopic intersections, which generally require approximation.

☆ The material in this paper was not presented at any conference. This paper was recommended for publication in revised form by Associate Editor Andrea Garulli under the direction of Editor Alessandro Chiuso.
* Corresponding author.
E-mail addresses: alesi@ufmg.br (A.A. de Paula), davide.raimondo@unipv.it (D.M. Raimondo), raffo@ufmg.br (G.V. Raffo), brunoot@ufmg.br (B.O.S. Teixeira).

The original paper on CZs (Scott, Raimondo, Marseglia, & Braatz, 2016) has focused on state estimation and fault diagnosis for state–space linear uncertain systems. The authors demonstrated that their state estimator achieves superior precision and detection rates compared to other guaranteed estimators (Alamo, Bravo, & Camacho, 2005; Chisci, Garulli, & Zappa, 1996), albeit with a slight increase in processing time. Encouraged by these advantages, the algorithm from Scott et al. (2016) has been expanded to encompass more general cases, as seen in Rego, Locatelli, Raimondo, and Raffo. Notably, recent contributions have extended CZs to address nonlinear systems, with Rego, Raffo, Scott, and Raimondo (2020), Rego et al. (2021) being notable examples. In Rego et al. (2020), the focus has been on linear output equations, while Rego et al. (2021) have further extended (Rego et al., 2020) to accommodate nonlinear measurement models and introduced a step to enforce algebraic equations on set-based estimates. These proposed algorithms have evolved from existing methods based on zonotopes, specifically, the mean value extension (Alamo et al., 2005) and first-order Taylor extension (Combastel, 2005).

All the aforementioned nonlinear methods rely on interval arithmetic to compute interval enclosures concerning the approximation remainder. Consequently, the algorithms proposed in Rego et al. (2020, 2021) still exhibit sensitivity to what is referred to as the wrapping and dependency effects. These effects encapsulate all the conservatism introduced by set-valued operations, with the dependency effect arising from the simultaneous occurrence of variables, while the remaining conservatism can be attributed to linear mappings and generalized intersections resulting from the wrapping effect (de Paula et al., 2022). An alternative approach to mitigate these interval-related issues is the utilization of the DC programming method, which involves approximating nonconvex mathematical programming problems using convex analysis tools (Tao & An, 1997).

In the context of set-membership filtering, Alamo, Bravo, Redondo, and Camacho (2008) has introduced approximate solutions for DC programming problems by supplying lower and upper bounds to enclose the global solutions. To accomplish this, the authors have replaced the *exact* minimization and maximization problems with *approximate* counterparts, the solutions of which can be determined by evaluating them at the vertices of a convex polytope. In accordance with this approach, Alamo et al. (2008) have modified the zonotopic filter from Alamo et al. (2005), which was originally based on mean value extension, to incorporate DC programming. In doing so, they have successfully mitigated the conservatism associated with the wrapping and dependency effects. It is worth noting that the methodology introduced in Alamo et al. (2008) differs from interval arithmetic in several aspects, including how it determines the range of nonlinear functions. Instead of using approximated functions and set-valued operations, it relies on convex components and real-valued operations.

Motivated by the advantages of DC programming over interval arithmetic and the superiority of CZs compared to zonotopes, we introduce a novel set-membership filter named CZDC. In contrast to Alamo et al. (2008), CZDC offers the following benefits: (i) utilizes CZs to represent both symmetric and asymmetric convex polytopes, surpassing the capabilities of zonotopes; (ii) utilizes the generalized intersection concept defined for CZs, resulting in improved precision and explicit calculations; (iii) enforces nonlinear equality constraints and linear inequality constraints on the state vector, leading to enhanced precision; and (iv) proposes a parallelotopic outer approximation for CZs, reducing the frequent need for interval hull calculations in solving DC programming problems. The aforementioned state constraints find relevance in various real-world applications, including compartmental systems (nonnegativity and conservation laws) (Teixeira, Chandrasekar, Tôrres, Aguirre, & Bernstein, 2009), unit-quaternion representations (holonomic constraints) (Rego et al., 2021), and water distribution networks (physical constraints and static relations) (Wang, Blesa, & Puig, 2017). It is essential to note that CZDC may entail a higher complexity level. CZs introduce additional representational elements, necessitating the development of specific algorithms for order reduction, interval hull computation, parallelotope calculation, and punctual estimation (Rego et al., 2020, 2021; Scott et al., 2016), and more. These operations are currently linked to linear program solvers, which account for the increased computational resource demand compared to Alamo et al. (2008). In contrast to de Paula et al. (2022), our present paper explores different aspects, albeit within a similar system framework. We focus on the class of CZs instead of zonotopes, address state nonlinear equality constraints and state inequality constraints represented as convex polytopes instead of zonotopes, and employ DC programming for approximation purposes, differing from the approaches presented in de Paula et al. (2022). Another significant difference lies in how the problems are approached and solved. Zonotopic problems typically require the solution of optimization problems, whereas state estimation using CZs primarily involves the concept of generalized intersection.

This paper is structured as follows: Section 2 formulates the state-estimation problem within the context of nonlinear state–space models that incorporate state constraints. Section 3 introduces a set of preliminary results. Section 4 provides a detailed presentation of the CZDC algorithm. In Section 5, CZDC is executed and compared against the algorithms from Alamo et al. (2008), Rego et al. (2021) using two numerical examples. Finally, Section 6 offers concluding remarks.

Notation

The set of natural numbers is denoted as $\mathbb{N}$. The set of positive integer numbers is denoted as $\mathbb{Z}_+$. The set of real numbers is denoted as $\mathbb{R}$. An $(n \times 1)$-dimensional vector and an $(n \times m)$-dimensional matrix are, respectively, denoted as $b \in \mathbb{R}^n$ and $A \in \mathbb{R}^{n\times m}$. An $(n \times m)$-dimensional zero matrix and an $(n \times n)$-dimensional identity matrix are, respectively, denoted as $0_{n\times m}$ and I_n. The transpose of a matrix and the diagonal matrix obtained from a vector are, respectively, denoted as $(\cdot)^\top$ and $\mathrm{diag}(\cdot)$. The ith row of a matrix is denoted as $(\cdot)_{i,:}$.

2. Problem statement

Consider the discrete-time nonlinear dynamical system

$$x_k = f\left(x_{k-1}, u_{k-1}, w_{k-1}\right), \tag{1}$$

$$y_k = h\left(x_k, v_k\right), \tag{2}$$

where $f : \mathbb{R}^n \times \mathbb{R}^p \times \mathbb{R}^q \to \mathbb{R}^n$ and $h : \mathbb{R}^n \times \mathbb{R}^r \to \mathbb{R}^m$ are the known process dynamics and measurement equations, respectively, $u_{k-1} \in \mathbb{R}^p$ is the known deterministic input vector, $y_k \in \mathbb{R}^m$ is the measured output vector, and $x_k \in \mathbb{R}^n$ is the state vector to be estimated. We assume that x_k satisfies the following nonlinear equality and linear inequality constraints:

$$g\left(x_k\right) = 0_{m_c\times 1}, \tag{3}$$

$$D_k x_k \le d_k, \tag{4}$$

where $g : \mathbb{R}^n \to \mathbb{R}^{m_c}$, $D_k \in \mathbb{R}^{n_c\times n}$, and $d_k \in \mathbb{R}^{n_c}$. Regarding (4), we make the following assumption to enable the direct use of convex polytopes.

Assumption 1. The inequality constraints given by (4), if present, define a compact feasibility set $\mathcal{X}_k^{\mathrm{F}} \subset \mathbb{R}^n$.

The process noise $w_{k-1} \in \mathbb{R}^q$, the measurement noise $v_k \in \mathbb{R}^r$, and the initial state $x_0 \in \mathbb{R}^n$ are bounded by convex polytopes $\mathcal{W}_{k-1}$, $\mathcal{V}_k$, and $\mathcal{X}_0$. Our set-membership filter aims at estimating the state vector x_k through convex polytopes $\mathcal{X}_k$ over $k \in \mathbb{Z}_+$. To achieve this goal at each k, given u_{k-1}, we define five steps as follows:

1. *Forecast*: $\mathcal{X}_{k|k-1} \supseteq \{f(x_{k-1}, u_{k-1}, w_{k-1}) : x_{k-1} \in \mathcal{X}_{k-1}, w_{k-1} \in \mathcal{W}_{k-1}\}$;
2. *Data assimilation*: $\breve{\mathcal{X}}_k \supseteq \left\{x_k \in \mathcal{X}_{k|k-1} : h(x_k, v_k) = y_k, v_k \in \mathcal{V}_k\right\}$;
3. *Admissibility*: $\check{\mathcal{X}}_k = \breve{\mathcal{X}}_k \cap \mathcal{X}_k^{\mathrm{F}}$;
4. *Consistency*: $\tilde{\mathcal{X}}_k \supseteq \left\{x_k \in \check{\mathcal{X}}_k : g(x_k) = 0_{m_c \times 1}\right\}$;
5. *Reduction*: $\mathcal{X}_k \supset \tilde{\mathcal{X}}_k$, with $\mathcal{X}_k$ being a set with lower complexity than $\tilde{\mathcal{X}}_k$.

Steps 1, 2, and 4 will be supported by a DC programming approach to obtain tight solutions. In steps 3 and 4, the state nonlinear equality and linear inequality constraints given by (3)–(4) are enforced on the estimator. Step 5 corresponds to a complexity reduction for convex polytopes, which is necessary to control the demand of computational resources; see Section 3 for further details.

3. Preliminaries

3.1. Constrained zonotopes

A constrained zonotope is defined as follows.

Definition 1 (*Scott et al., 2016*). Let $G^{\mathrm{x}} \in \mathbb{R}^{n \times n_g}$ be the generator matrix, $c^{\mathrm{x}} \in \mathbb{R}^n$ the center, $A^{\mathrm{x}} \in \mathbb{R}^{n_h \times n_g}$ the constraint matrix, and $b^{\mathrm{x}} \in \mathbb{R}^{n_h}$ the constraint vector. Let also $\mathcal{B}^{n_g} \triangleq [-1, 1]^{n_g}$ be the unitary box of dimension n_g, and $\mathcal{B}(A^{\mathrm{x}}, b^{\mathrm{x}}) \triangleq \{\xi \in \mathcal{B}^{n_g} : A^{\mathrm{x}}\xi = b^{\mathrm{x}}\}$ the constrained unitary box. Then, the CZ $\mathcal{X} \subset \mathbb{R}^n$ is defined as

$$\mathcal{X} \triangleq \left\{G^{\mathrm{x}}, c^{\mathrm{x}}, A^{\mathrm{x}}, b^{\mathrm{x}}\right\} = \left\{G^{\mathrm{x}}\xi + c^{\mathrm{x}} : \xi \in \mathcal{B}\left(A^{\mathrm{x}}, b^{\mathrm{x}}\right)\right\}. \quad (5)$$

The terms n_g and n_h refer to the number of generators and constraints, respectively. For zonotopes, A^{x} and b^{x} do not exist. In this case, the notation is abbreviated to $\mathcal{X} = \{G^{\mathrm{x}}, c^{\mathrm{x}}\}$.

Let $m \in \mathbb{R}^r$, $L \in \mathbb{R}^{r \times n}$, $\mathcal{Y} = \{G^{\mathrm{y}}, c^{\mathrm{y}}, A^{\mathrm{y}}, b^{\mathrm{y}}\} \subset \mathbb{R}^n$, $\mathcal{W} = \{G^{\mathrm{w}}, c^{\mathrm{w}}, A^{\mathrm{w}}, b^{\mathrm{w}}\} \subset \mathbb{R}^p$, and $M \in \mathbb{R}^{p \times n}$. The affine transformation, Minkowski sum, generalized intersection, and Cartesian product of CZs are *explicitly* computed as, respectively,

$$L\mathcal{X} \oplus m = \left\{LG^{\mathrm{x}}, \left(Lc^{\mathrm{x}} + m\right), A^{\mathrm{x}}, b^{\mathrm{x}}\right\}, \quad (6)$$

$$\mathcal{X} \oplus \mathcal{Y} = \left\{\begin{bmatrix} G^{\mathrm{x}} & G^{\mathrm{y}} \end{bmatrix}, (c^{\mathrm{x}} + c^{\mathrm{y}}), \begin{bmatrix} A^{\mathrm{x}} & 0_{n_h \times n_g^{\mathrm{y}}} \\ 0_{n_h^{\mathrm{y}} \times n_g} & A^{\mathrm{y}} \end{bmatrix}, \begin{bmatrix} b^{\mathrm{x}} \\ b^{\mathrm{y}} \end{bmatrix}\right\}, \quad (7)$$

$$\mathcal{X} \cap_M \mathcal{W} = \left\{\begin{bmatrix} G^{\mathrm{x}} & 0_{n \times n_g^{\mathrm{w}}} \end{bmatrix}, c^{\mathrm{x}}, \begin{bmatrix} A^{\mathrm{x}} & 0_{n_h \times n_g^{\mathrm{w}}} \\ 0_{n_h^{\mathrm{w}} \times n_g} & A^{\mathrm{w}} \\ MG^{\mathrm{x}} & -G^{\mathrm{w}} \end{bmatrix}, \begin{bmatrix} b^{\mathrm{x}} \\ b^{\mathrm{w}} \\ c^{\mathrm{w}} - Mc^{\mathrm{x}} \end{bmatrix}\right\}, \quad (8)$$

$$\mathcal{X} \times \mathcal{W} = \left\{\begin{bmatrix} G^{\mathrm{x}} & 0_{n \times n_g^{\mathrm{w}}} \\ 0_{n^{\mathrm{w}} \times n_g} & G^{\mathrm{w}} \end{bmatrix}, \begin{bmatrix} c^{\mathrm{x}} \\ c^{\mathrm{w}} \end{bmatrix}, \begin{bmatrix} A^{\mathrm{x}} & 0_{n_h \times n_g^{\mathrm{w}}} \\ 0_{n_h^{\mathrm{w}} \times n_g} & A^{\mathrm{w}} \end{bmatrix}, \begin{bmatrix} b^{\mathrm{x}} \\ b^{\mathrm{w}} \end{bmatrix}\right\}. \quad (9)$$

For brevity, $M = \mathrm{I}_n$ will be omitted in "$\cap$". Note that the set operations (7)–(9) imply increase of the number of constraints n_h and generators n_g for CZs. These values can be reduced to desired quantities φ_c and φ_g, as done in Scott et al. (2016), at the price of conservativeness (outer approximation). The following result is used to obtain the so-called *interval hull* of a CZ $\mathcal{X}$, $\square\mathcal{X} = \left[\zeta^{\mathrm{L}}, \zeta^{\mathrm{U}}\right]$, such that $\mathcal{X} \subseteq \square\mathcal{X}$.

Proposition 1 (*Rego et al., 2020*). *Let $\mathcal{X} = \{G^{\mathrm{x}}, c^{\mathrm{x}}, A^{\mathrm{x}}, b^{\mathrm{x}}\} \subset \mathbb{R}^n$. The interval hull $\left[\zeta^{\mathrm{L}}, \zeta^{\mathrm{U}}\right] \supseteq \mathcal{X}$ is obtained by solving linear programs for each $i = 1, \ldots, n$:*

$$\zeta_i^{\mathrm{L}} \triangleq \min_{\xi} \left\{G_{i,:}^{\mathrm{x}}\xi + c_i^{\mathrm{x}} : \xi \in \mathcal{B}\left(A^{\mathrm{x}}, b^{\mathrm{x}}\right)\right\}, \ i = 1, \ldots, n,$$

$$\zeta_i^{\mathrm{U}} \triangleq \max_{\xi} \left\{G_{i,:}^{\mathrm{x}}\xi + c_i^{\mathrm{x}} : \xi \in \mathcal{B}\left(A^{\mathrm{x}}, b^{\mathrm{x}}\right)\right\}, \ i = 1, \ldots, n.$$

As any box expressed in interval arithmetic, the interval hull of a CZ can be equivalently expressed in affine arithmetic doing $\square\mathcal{X} = \{\mathrm{diag}(\mathrm{rad}(\square\mathcal{X})), \mathrm{mid}(\square\mathcal{X})\}$, where $\mathrm{rad}(\square\mathcal{X}) \triangleq \frac{1}{2}\left(\zeta^{\mathrm{U}} - \zeta^{\mathrm{L}}\right)$ and $\mathrm{mid}(\square\mathcal{X}) \triangleq \frac{1}{2}\left(\zeta^{\mathrm{L}} + \zeta^{\mathrm{U}}\right)$. For interval matrices $[M] = \left\{M \in \mathbb{R}^{n \times m} : M^{\mathrm{L}} \leq M \leq M^{\mathrm{U}}\right\}$, we have $\mathrm{rad}([M]) = \frac{1}{2}\left(M^{\mathrm{U}} - M^{\mathrm{L}}\right)$ and $\mathrm{mid}([M]) = \frac{1}{2}\left(M^{\mathrm{L}} + M^{\mathrm{U}}\right)$, with M^{L} and M^{U} being known matrices with different values $M_{i,j}^{\mathrm{L}}$ and $M_{i,j}^{\mathrm{U}}$, respectively, for $i = 1, \ldots, n$ and $j = 1, \ldots, m$.

3.2. DC programming

As shown in Rego et al. (2021), (6)–(8) can be directly employed in state estimation when f, h, and g given by (1), (2), and (3) are linear. Conversely, the nonlinear case requires some approximation of such functions to enable the use of (6)–(8). Contributions to this topic have been proposed in Rego et al. (2021, Lemmas 1 and 2) using CZs.

In this paper, a DC programming approach is used to compute linearization enclosures. This approach is convenient to reduce conservatism in comparison with interval methods based on Lagrange remainder as those proposed in Althoff, Stursberg, and Buss (2008), Combastel (2005), which concentrate the linearization error in the quadratic term of a truncated Taylor series. Next, we present definitions and results related to DC programming.

Definition 2 (*Alamo et al., 2008*). Consider a polytope $\mathcal{P} \subset \mathbb{R}^n$ and a function $\varrho : \mathbb{R}^n \to \mathbb{R}^m$. If ϱ can be rewritten as the difference between two convex functions ϱ^{a} and ϱ^{b} in $\mathcal{P}$, then, ϱ is called DC on $\mathcal{P}$.

Definition 3 (*Alamo et al., 2008*). Consider that the function $\varrho : \mathbb{R}^n \to \mathbb{R}^m$ is DC on $\mathcal{P} \subset \mathbb{R}^n$, with ϱ^{a} and ϱ^{b} being its DC components such that $\varrho(z) = \varrho^{\mathrm{a}}(z) - \varrho^{\mathrm{b}}(z)$. Then, for each component $i = 1, \ldots, m$, the ith DC programming problems are formulated as

$$\min_{z \in \mathcal{P}} \varrho_i(z), \quad \max_{z \in \mathcal{P}} \varrho_i(z). \quad (10)$$

Definition 4 (*Alamo et al., 2008*). Let $\varrho(z) = \left(\varrho^{\mathrm{a}}(z) - \varrho^{\mathrm{b}}(z)\right) \in \mathbb{R}^m$ be DC on $\mathcal{P} \subset \mathbb{R}^n$. Then, the linear minorant of ϱ^{s}, with $\mathrm{s} = \{\mathrm{a}, \mathrm{b}\}$, is defined as

$$\bar{\varrho}^{\mathrm{s}}(z) \triangleq \varrho^{\mathrm{s}}(\bar{z}) + F^{\mathrm{s}}(z - \bar{z}), \quad (11)$$

where

$$F^{\mathrm{s}} \triangleq \nabla_z \varrho^{\mathrm{s}}(\bar{z}) = \begin{bmatrix} \frac{\partial \varrho_1^{\mathrm{s}}}{\partial z_1} & \cdots & \frac{\partial \varrho_1^{\mathrm{s}}}{\partial z_n} \\ \vdots & \ddots & \vdots \\ \frac{\partial \varrho_m^{\mathrm{s}}}{\partial z_1} & \cdots & \frac{\partial \varrho_m^{\mathrm{s}}}{\partial z_n} \end{bmatrix}\Bigg|_{\bar{z}} \quad (12)$$

is the Jacobian matrix evaluated at some $\bar{z} \in \mathcal{P}$. The term *minorant* comes from the convexity of ϱ^{s} that implies the inequalities $\varrho^{\mathrm{s}}(z) \geq \bar{\varrho}^{\mathrm{s}}(z)$, $\forall z \in \mathcal{P}$.

Proposition 2 (*Alamo et al., 2008*). *Let $\varrho(z) = \left(\varrho^{\mathrm{a}}(z) - \varrho^{\mathrm{b}}(z)\right) \in \mathbb{R}^m$ be a DC function on the polytope $\mathcal{P} \subset \mathbb{R}^n$. Then, according to Definition 4, the following inequalities hold:*

$$\min_{z \in \mathcal{P}} \varrho_i(z) \geq \min_{z \in \mathrm{vert}(\mathcal{P})} \bar{\varrho}_i^{\mathrm{a}}(z) - \varrho_i^{\mathrm{b}}(z), \quad (13)$$

$$\max_{z\in\mathcal{P}} \varrho_i(z) \le \max_{z\in\text{vert}(\mathcal{P})} \varrho_i^{\text{a}}(z) - \bar{\varrho}_i^{\text{b}}(z), \tag{14}$$

for $i = 1, \ldots, m$, with $\text{vert}(\mathcal{P})$ being the set of vertices of $\mathcal{P}$, with $\bar{\varrho}_i^{\text{a}}(z) - \varrho_i^{\text{b}}(z)$ being a concave function, and with $\varrho_i^{\text{a}}(z) - \bar{\varrho}_i^{\text{b}}(z)$ being a convex function.

In order to control the number of vertices, and thereby, the computational cost associated to (13)–(14), we outer approximate the polytope $\mathcal{P}$ by either its interval hull $\square\mathcal{P} \supseteq \mathcal{P}$ or a parallelotope $\mathcal{T} \supseteq \mathcal{P}$, since these representations involve 2^n vertices. Polytopes are here represented by CZs. Therefore, the interval hull $\square\mathcal{P}$ is obtained with Proposition 1. In order to obtain a tight parallelotope $\mathcal{T}$ to polytope $\mathcal{P}$, we next propose a new result, in which a candidate parallelotope $\mathcal{C} \supseteq \mathcal{P}$ is tightened via linear programs. The set $\mathcal{C}$ is here computed as in Remark 1.

Remark 1. If all constraints and generators of a CZ $\mathcal{P}$ are reduced with Method 4 of Yang and Scott (2018), then a parallelotope $\mathcal{C} \supset \mathcal{P}$ is obtained.

Proposition 3. *Let $\mathcal{C} = \{G^{\text{c}}, c^{\text{c}}\} \subset \mathbb{R}^n$ be a parallelotope containing the CZ $\mathcal{P} = \{G^{\text{z}}, c^{\text{z}}, A^{\text{z}}, b^{\text{z}}\} \subset \mathbb{R}^n$. By solving the linear programs*

$$\zeta_i^{\text{L}} = \min_{\xi^{\text{c}},\xi^{\text{z}}} \left\{\xi_i^{\text{c}} : G_{i,:}^{\text{c}}\xi^{\text{c}} + c_i^{\text{c}} = G_{i,:}^{\text{z}}\xi^{\text{z}} + c_i^{\text{z}}, \xi^{\text{c}} \in \mathcal{B}^n, \xi^{\text{z}} \in \mathcal{B}\left(A^{\text{z}}, b^{\text{z}}\right)\right\},$$

$$\zeta_i^{\text{U}} = \max_{\xi^{\text{c}},\xi^{\text{z}}} \left\{\xi_i^{\text{c}} : G_{i,:}^{\text{c}}\xi^{\text{c}} + c_i^{\text{c}} = G_{i,:}^{\text{z}}\xi^{\text{z}} + c_i^{\text{z}}, \xi^{\text{c}} \in \mathcal{B}^n, \xi^{\text{z}} \in \mathcal{B}\left(A^{\text{z}}, b^{\text{z}}\right)\right\},$$

for $i = 1, \ldots, n$, we obtain the parallelotope
$\mathcal{T} = \left\{G^{\text{c}}\text{diag}\left(\text{rad}\left(\left[\zeta^{\text{L}}, \zeta^{\text{U}}\right]\right)\right), c^{\text{c}} + G^{\text{c}}\text{mid}\left(\left[\zeta^{\text{L}}, \zeta^{\text{U}}\right]\right)\right\} \supseteq \mathcal{P}.$

Proof. Given the parallelotope $\mathcal{C} \supseteq \mathcal{P}$, a new parallelotope $\mathcal{T}$ is investigated. The set $\mathcal{T}$ must be an outer approximation of $\mathcal{P}$ containing or being equal to $\mathcal{C}$. To achieve that, both the generator matrix G^{c} and the center c^{c} of $\mathcal{C}$ are firstly fixed. After, the slack variable $\xi^{\text{c}} \in \mathcal{B}^n$ is manipulated to tighten the facets of $\mathcal{C}$ onto the CZ $\mathcal{P}$. This strategy implies $2n$ linear programs with $G_{i,:}^{\text{c}}\xi^{\text{c}} + c_i^{\text{c}} = G_{i,:}^{\text{z}}\xi^{\text{z}} + c_i^{\text{z}}$ being the ith linear equality constraint, where $i = 1, \ldots, n$ and $\xi^{\text{z}} \in \mathcal{B}(A^{\text{z}}, b^{\text{z}})$. Since the minimization and maximization of ξ_i^{c} yield the smallest possible box $\left[\zeta^{\text{L}}, \zeta^{\text{U}}\right] \subset \mathcal{B}^n$, we guarantee that $\mathcal{T} \subseteq \mathcal{C}$. Then, $\mathcal{T} = G^{\text{c}}\left[\zeta^{\text{L}}, \zeta^{\text{U}}\right] \oplus c^{\text{c}}$ is a parallelotopic outer approximation of $\mathcal{P}$, which can be rewritten as a zonotope using a rescaling (see $\mathcal{T}$ in the statement of Proposition 3). ■

A procedure to compute the DC decomposition of a function ϱ is presented in Proposition 4.

Proposition 4 (*Adapted from Adjiman and Floudas (1996), Alamo et al. (2008)*)**.** *Let $\varrho : \mathbb{R}^n \times \mathbb{R}^p \to \mathbb{R}^m$ be a function of class $\mathcal{C}^2$ in $\mathcal{P}$ and with deterministic input $u \in \mathbb{R}^p$, and $\square\mathcal{P} \subset \mathbb{R}^n$ be the interval hull of $\mathcal{P}$. Consider functions $\varrho_i^{\text{a}}(z, u) = \varrho_i(z, u) + \varrho_i^{\text{b}}(z)$ and $\varrho_i^{\text{b}}(z) = \dfrac{\tilde{\lambda}_i}{2}z^\top z$, for $i = 1, \ldots, m$, where*

$$\tilde{\lambda}_i = \max\left\{0, -\breve{\lambda}_i\right\}, \tag{15}$$

with $\breve{\lambda}_i \in \mathbb{R}$ being computed as in Adjiman and Floudas (1996, Equation (12)), which is a lower bound for the smallest eigenvalue of interval Hessian matrix $[H_i] = (\partial^2/\partial z^2)\varrho_i(\square\mathcal{P}, u)$. Then, $\varrho = \varrho^{\text{a}} - \varrho^{\text{b}}$ is a DC function on $\square\mathcal{P}$.

Proof. This proof follows the same discussion presented in Alamo et al. (2008, Section 3), with the difference being the introduction of the deterministic input u. ■

Remark 2. Each function ϱ_i^{b} could be defined with $\frac{1}{2}z^\top Q_i z$, where Q_i is a diagonal matrix whose elements could be obtained via semidefinite programming. Moreover, instead of convexifying ϱ (obtaining ϱ^{a}), we could convexify $-\varrho$ and place this result in ϱ^{b}.

4. The novel state estimator

Next, we present the novel set-membership filter based on CZs and DC programming, called CZDC. This algorithm solves the problem formulated in Section 2 in five steps. The general idea is to firstly linearize models. Then, operations (6)–(8) are performed on the linearized models. Finally, DC programming is employed to bound the linearization error.

In order to obtain linearization error enclosures $\mathcal{R}$, we present Lemma 1. For practical reasons, the input CZ $\mathcal{Z}$ may be outer approximated by either a box $\square\mathcal{Z}$ (Proposition 1) or a parallelotope $\mathcal{T}$ (Proposition 3), yielding the desired polytope $\mathcal{P}$, before solving the problems (17)–(18).

Lemma 1 (*Adapted from Alamo et al. (2008)*)**.** *Let $\varrho : \mathbb{R}^n \times \mathbb{R}^p \to \mathbb{R}^m$ be a function in the CZ $\mathcal{Z}$ and with deterministic input $u \in \mathbb{R}^p$, whose first-order expansion is given by*

$$\bar{\varrho}(z, u) = \varrho\left(\bar{z}, u\right) + F\left(z - \bar{z}\right), \tag{16}$$

where $F = \nabla_z\varrho(\bar{z}, u)$, $\bar{z} \in \mathcal{P}$ is any punctual estimate, and $\mathcal{P} \supseteq \mathcal{Z}$ is a convex polytope. Let $e(z, u) \triangleq \varrho(z, u) - \bar{\varrho}(z, u)$ be the linearization error. Let also ϱ^{a} and ϱ^{b} be convex functions such that $\varrho = \varrho^{\text{a}} - \varrho^{\text{b}}$ is DC on $\mathcal{P}$. Finally, let $\left(\varrho^{\text{a}} - \bar{\varrho}^{\text{b}} - \bar{\varrho}\right)$ be a convex majorant of e, and let $\left(\bar{\varrho}^{\text{a}} - \varrho^{\text{b}} - \bar{\varrho}\right)$ be a concave minorant of e. Then, according to Proposition 2, a linearization enclosure $\mathcal{R} = \left[e^-, e^+\right] \ni e$ is given by

$$e_i^- = \min_{z\in\text{vert}(\mathcal{P})} \left(\bar{\varrho}_i^{\text{a}}(z, u) - \varrho_i^{\text{b}}(z, u) - \bar{\varrho}_i(z, u)\right), \tag{17}$$

$$e_i^+ = \max_{z\in\text{vert}(\mathcal{P})} \left(\varrho_i^{\text{a}}(z, u) - \bar{\varrho}_i^{\text{b}}(z, u) - \bar{\varrho}_i(z, u)\right), \tag{18}$$

for $i = 1, \ldots, m$. Once (17)–(18) are solved, the intervals are expressed as the zonotope $\mathcal{R} = \{G^{\text{e}}, c^{\text{e}}\}$ with

$$G^{\text{e}} = \text{diag}\left(\text{rad}\left(\left[e^-, e^+\right]\right)\right), \tag{19}$$

$$c^{\text{e}} = \text{mid}\left(\left[e^-, e^+\right]\right). \tag{20}$$

Proof. This proof is similar to Alamo et al. (2008, Proof of Lemma 1), with the difference being that $\mathcal{Z}$ is a CZ (instead of zonotope), and ϱ is any DC function in $\mathcal{P}$ and with deterministic input u. ■

Remark 3. In Lemma 1, the variable u is different from the uncertain variable z because it is deterministic (or a singleton). Then, the linearization of ϱ with respect to u is zero. It means that z is actually responsible by the uncertainty of e.

In the following, the results to execute a loop of CZDC are presented, which were inspired from Rego et al. (2021).

Theorem 1 (*Forecast Step*)**.** *Consider the CZs $\mathcal{X}_{k-1} \subset \mathbb{R}^n$ and $\mathcal{W}_{k-1} \subset \mathbb{R}^q$, and the deterministic input $u_{k-1} \in \mathbb{R}^p$. Let $f : \mathbb{R}^n \times \mathbb{R}^p \times \mathbb{R}^q \to \mathbb{R}^n$ (1) be rewritten as $\varrho^{\text{f}} : \mathbb{R}^{(n+q)} \times \mathbb{R}^p \to \mathbb{R}^n$ using the augmented vector $z_{k-1} = \left[x_{k-1}^\top \quad w_{k-1}^\top\right]^\top$. Let also $\varrho^{\text{f}} = \varrho^{\text{fa}} - \varrho^{\text{fb}}$ be DC on the polytope $\mathcal{P}_{k-1} \supseteq \mathcal{Z}_{k-1} = \mathcal{X}_{k-1} \times \mathcal{W}_{k-1}$. Finally, let $\mathcal{R}_{k-1} \subset \mathbb{R}^n$ be the set returned by Lemma 1 to enclose the linearization error of ϱ^{f} for a given punctual estimate $\bar{z} \in \mathcal{P}_{k-1}$. Then, the exact image $\varrho^{\text{f}}(\mathcal{Z}_{k-1}, u_{k-1})$ is outer approximated by the CZ*

$$\mathcal{X}_{k|k-1} = \left(\varrho^{\text{f}}(\bar{z}, u_{k-1}) - F\bar{z}\right) \oplus F\mathcal{Z}_{k-1} \oplus \mathcal{R}_{k-1}, \tag{21}$$

with $F = \nabla_z\varrho^{\text{f}}(\bar{z}, u_{k-1})$ being the Jacobian matrix evaluated at $\bar{z} = \left[\bar{x}^\top \quad \bar{w}^\top\right]^\top$.

Proof. This proof is similar to Alamo et al. (2008, Proof of Theorem 1), with the difference being the propagation of CZs instead of zonotopes, and the introduction of deterministic input u_{k-1}. ■

Theorem 2 (*Data-Assimilation Step*)**.** *Consider the CZs $\mathcal{X}_{k|k-1} \subset \mathbb{R}^n$ and $\mathcal{V}_k \subset \mathbb{R}^r$, and the measured output $y_k \in \mathbb{R}^m$. Let $h : \mathbb{R}^n \times \mathbb{R}^r \to \mathbb{R}^m$ (2) be rewritten as $\varrho^{\mathrm{h}} : \mathbb{R}^{(n+r)} \to \mathbb{R}^m$ using the augmented vector $z_k = \begin{bmatrix} x_k^\top & v_k^\top \end{bmatrix}^\top$. Let also $\varrho^{\mathrm{h}} = \varrho^{\mathrm{ha}} - \varrho^{\mathrm{hb}}$ be DC on the polytope $\mathcal{P}_k \supseteq \mathcal{Z}_k = \mathcal{X}_{k|k-1} \times \mathcal{V}_k$. Finally, let $\mathcal{R}_k \subset \mathbb{R}^m$ be the set returned by Lemma 1 to enclose the linearization error of ϱ^{h} for a given punctual estimate $\bar{z} \in \mathcal{P}_k$. Then, the exact set $\left\{x_k \in \mathcal{X}_{k|k-1} : y_k = h\left(x_k, v_k\right), v_k \in \mathcal{V}_k\right\}$ is over approximated by the CZ*

$$\check{\mathcal{X}}_k = \mathcal{X}_{k|k-1} \cap_{H^{\mathrm{x}}} \mathcal{Y}_k, \tag{22}$$

where $\mathcal{Y}_k = \left(y_k - \varrho^{\mathrm{h}}(\bar{z}) + H\bar{z}\right) \oplus (-H^{\mathrm{v}}\mathcal{V}_k) \oplus (-\mathcal{R}_k)$, with $H = \begin{bmatrix} H^{\mathrm{x}} & H^{\mathrm{v}} \end{bmatrix}$, $H^{\mathrm{x}} = \nabla_x \varrho^{\mathrm{h}}(\bar{z})$, and $H^{\mathrm{v}} = \nabla_v \varrho^{\mathrm{h}}(\bar{z})$.

Proof. Let

$$y_k = \varrho^{\mathrm{h}}(\bar{z}) + H\left(z_k - \bar{z}\right) + e_k^{\mathrm{h}}$$

be the analytical linearization of the DC function $\varrho^{\mathrm{h}} = \varrho^{\mathrm{ha}} - \varrho^{\mathrm{hb}}$ on $\mathcal{P}_k$, and let the CZ $\mathcal{R}_k \ni e_k^{\mathrm{h}}$ be the linearization error enclosure given by Lemma 1. By making explicit the term $H^{\mathrm{x}}x_k$ from $Hz_k = \begin{bmatrix} H^{\mathrm{x}} & H^{\mathrm{v}} \end{bmatrix} \begin{bmatrix} x_k \\ v_k \end{bmatrix}$, we obtain $H^{\mathrm{x}}x_k = y_k - \varrho^{\mathrm{h}}(\bar{z}) + H\bar{z} - H^{\mathrm{v}}v_k - e_k^{\mathrm{h}}$, which implies the CZ $\mathcal{Y}_k = \left(y_k - \varrho^{\mathrm{h}}(\bar{z}) + H\bar{z}\right) \oplus (-H^{\mathrm{v}}\mathcal{V}_k) \oplus (-\mathcal{R}_k)$. Then, we employ the generalized inter Eq. (8) to match $\mathcal{X}_{k|k-1}$ with $\mathcal{Y}_k$, yielding $\check{\mathcal{X}}_k$. ■

Remark 4. If functions f and h are affine in the noise terms w_{k-1} and v_k, respectively, then these terms are canceled during the computation of $\mathcal{R}$ in Theorems 1 and 2. It means that, instead of $2^{(n+q)}$ and $2^{(n+r)}$ vertices, we need to process 2^n vertices only.

The consistency step enforces the nonlinear invariants described in (3). In algebraic terms, (3) is a special case of (2). Then, the consistency step is a direct consequence from Theorem 2, being next presented as a corollary. For brevity, the admissibility step is presented together with the consistency one.

Corollary 1 (*Consistency Step*)**.** *Consider the CZ $\check{\mathcal{X}}_k \subset \mathbb{R}^n$ (Theorem 2) and the feasible set $\mathcal{X}_k^{\mathrm{F}} \subset \mathbb{R}^n$. Let $\check{\mathcal{X}}_k = \check{\mathcal{X}}_k \cap \mathcal{X}_k^{\mathrm{F}}$ be the admissible set (admissibility step in Section 2). Let $g : \mathbb{R}^n \to \mathbb{R}^{m_c}$ (3) be rewritten as $g = g^{\mathrm{a}} - g^{\mathrm{b}}$, where g^{a} and g^{b} are convex functions in the polytope $\check{\mathcal{P}}_k \supseteq \check{\mathcal{X}}_k$. Let also $\mathcal{R}_k \subset \mathbb{R}^{m_c}$ be the set returned by Lemma 1 to enclose the linearization error of g for a given punctual estimate $\bar{x} \in \check{\mathcal{P}}_k$. Then, the exact set $\left\{x_k \in \check{\mathcal{X}}_k : g\left(x_k\right) = 0_{m_c \times 1}\right\}$ is over approximated by the CZ*

$$\tilde{\mathcal{X}}_k = \check{\mathcal{X}}_k \cap_H \mathcal{C}_k, \tag{23}$$

where $H = \nabla_x g(\bar{x})$ and $\mathcal{C}_k = (-g(\bar{x}) + H\bar{x}) \oplus (-\mathcal{R}_k)$.

Proof. This proof is similar to the proof of Theorem 2, whose difference is the replacement of y_k, h, and z_k by $0_{m_c \times 1}$, g, and x_k, respectively. ■

We summarize the steps of CZDC in Algorithm 1.

Algorithm 1: $\mathcal{X}_k = \mathrm{CZDC}\big(f, f^{\mathrm{a}}, f^{\mathrm{b}}, \mathcal{X}_{k-1}, u_{k-1}, \mathcal{W}_{k-1}, y_k, h, h^{\mathrm{a}}, h^{\mathrm{b}}, \mathcal{V}_k, g, g^{\mathrm{a}}, g^{\mathrm{b}}, \mathcal{X}_k^{\mathrm{F}}, \varphi_c, \varphi_g\big)$

1 Apply Theorem 1 to obtain the CZ $\mathcal{X}_{k|k-1}$
2 Apply Theorem 2 to obtain the CZ $\check{\mathcal{X}}_k$
3 Compute $\check{\mathcal{X}}_k = \check{\mathcal{X}}_k \cap \mathcal{X}_k^{\mathrm{F}}$
4 Apply Corollary 1 to obtain the CZ $\tilde{\mathcal{X}}_k$
5 Apply the steps of (i) rescaling, (ii) preconditioning, (iii) elimination of constraints and (partial) generators, and (iv) elimination of generators proposed in Scott et al. (2016) to reduce the number of constraints n_h and generators n_g of $\tilde{\mathcal{X}}_k$ to φ_c and φ_g, respectively, yielding the CZ $\mathcal{X}_k$

Remark 5. We recall that DC programming is motivated to mitigate the wrapping and dependency effects related to interval arithmetic, but its computational challenge (control and manipulation of vertices) is transmitted to CZDC. Besides, the fact of CZs demanding solvers of linear programs, to compute interval hulls and parallelotopes for instance, may become the CZDC more costly than the algorithm of Alamo et al. (2008).

4.1. Complexity analysis

The worst-case computational complexity $O(\cdot)$ for each step of CZDC (Algorithm 1) is shown in Table 1. Such complexities were derived using basic operations among CZs (Rego et al., 2020). Regarding the forecast, data assimilation, and consistency steps, the complexity order to obtain the linearization point $\bar{z}$ is not included since it depends on the employed methodology. As in Rego et al. (2020), we also assume that the evaluation of nonlinear functions has complexity $O(1)$. In the second column of Table 1, the cubic term between parenthesis refers to either the computation of parallelotope via linear programs or the order reduction. The term $2^{\bar{n}}$ is related to either the computation of vertices or the DC programming problems (17)–(18). In turn, the third column of Table 1 presents the amount of constraints and generators for the state CZ $\mathcal{X}$ over the different steps.

Table 1 makes the following assumptions: $\mathcal{X}_{k-1} = \left\{G_{k-1}^{\mathrm{x}}, c_{k-1}^{\mathrm{x}}, A_{k-1}^{\mathrm{x}}, b_{k-1}^{\mathrm{x}}\right\} \subset \mathbb{R}^n$, $\mathcal{W}_{k-1} = \left\{G_{k-1}^{\mathrm{w}}, c_{k-1}^{\mathrm{w}}, A_{k-1}^{\mathrm{w}}, b_{k-1}^{\mathrm{w}}\right\} \subset \mathbb{R}^q$, $\mathcal{V}_k = \left\{G_k^{\mathrm{v}}, c_k^{\mathrm{v}}, A_k^{\mathrm{v}}, b_k^{\mathrm{v}}\right\} \subset \mathbb{R}^r$, and $\mathcal{X}_k^{\mathrm{F}} = \left\{G_k^{\mathrm{x^F}}, c_k^{\mathrm{x^F}}, A_k^{\mathrm{x^F}}, b_k^{\mathrm{x^F}}\right\} \subset \mathbb{R}^n$, where $G_{k-1}^{\mathrm{x}} \in \mathbb{R}^{n \times n_g}$, $G_{k-1}^{\mathrm{w}} \in \mathbb{R}^{q \times n_g^{\mathrm{w}}}$, $G_k^{\mathrm{v}} \in \mathbb{R}^{r \times n_g^{\mathrm{v}}}$, $G_k^{\mathrm{x^F}} \in \mathbb{R}^{n \times n_g^{\mathrm{x^F}}}$, $c_{k-1}^{\mathrm{x}} \in \mathbb{R}^n$, $c_{k-1}^{\mathrm{w}} \in \mathbb{R}^q$, $c_k^{\mathrm{v}} \in \mathbb{R}^r$, $c_k^{\mathrm{x^F}} \in \mathbb{R}^n$, $A_{k-1}^{\mathrm{x}} \in \mathbb{R}^{n_h \times n_g}$, $A_{k-1}^{\mathrm{w}} \in \mathbb{R}^{n_h^{\mathrm{w}} \times n_g^{\mathrm{w}}}$, $A_k^{\mathrm{v}} \in \mathbb{R}^{n_h^{\mathrm{v}} \times n_g^{\mathrm{v}}}$, $A_k^{\mathrm{x^F}} \in \mathbb{R}^{n_h^{\mathrm{x^F}} \times n_g^{\mathrm{x^F}}}$, $b_{k-1}^{\mathrm{x}} \in \mathbb{R}^{n_h}$, $b_{k-1}^{\mathrm{w}} \in \mathbb{R}^{n_h^{\mathrm{w}}}$, $b_k^{\mathrm{v}} \in \mathbb{R}^{n_h^{\mathrm{v}}}$, and $b_k^{\mathrm{x^F}} \in \mathbb{R}^{n_h^{\mathrm{x^F}}}$. These sets are evaluated over the functions $f : \mathbb{R}^n \times \mathbb{R}^p \times \mathbb{R}^q \to \mathbb{R}^n$, $h : \mathbb{R}^n \times \mathbb{R}^r \to \mathbb{R}^m$, and $g : \mathbb{R}^n \to \mathbb{R}^{m_c}$, considering the vectors $u_{k-1} \in \mathbb{R}^p$ and $y_k \in \mathbb{R}^m$. At the end of an iteration of CZDC, the desired CZ $\mathcal{X}_k$ is returned with φ_c constraints and φ_g generators.

Remark 6. According to Table 1, the output CZs obtained by Theorems 1–2 and Corollary 1 have smaller number of constraints and generators than those pointed out by Remarks 5, 7, and 10 from Rego et al. (2021). Exceptionally, the number of constraints for $\mathcal{X}_{k|k-1}$ coincides with the value indicated in Rego et al. (2021, Remark 5) for the CZMV algorithm. Then, although CZDC seems more costly due to the quantity of operations, the achieved smallest number of constraints and generators may compensate the final performance in comparison with CZMV and CZFO.

5. Numerical results

In this section, CZDC is experimented over two case studies. For comparison purposes, we also implement the state-of-the-art algorithms proposed in Rego et al. (2021), called CZFO (based on Taylor expansion) and CZMV (based on mean value extension).

Table 1
Complexity order of the forecast, data assimilation, admissibility, consistency, and reduction steps from CZDC using Proposition 3.

Step	$O(\cdot)$	Definition
Forecast	$\tilde{n}_h(\tilde{n}_h+\tilde{n}_g)^3+\tilde{n}(\tilde{n}+\tilde{n}_g)(\tilde{n}+\tilde{n}_h+\tilde{n}_g)^3+\tilde{n}^2 2^{\tilde{n}}$	$\tilde{n}=n+q$, $\tilde{n}_h=n_h+n_h^{\mathrm{w}}$, $\tilde{n}_g=n_g+n_g^{\mathrm{w}}$
Data assimilation	$\tilde{n}_h(\tilde{n}_h+\tilde{n}_g)^3+\tilde{n}(\tilde{n}+\tilde{n}_g)(\tilde{n}+\tilde{n}_h+\tilde{n}_g)^3$ $+(\tilde{n}^2+m)2^{\tilde{n}}+mrn_g^{\mathrm{v}}+mn(\tilde{n}_g-n_g^{\mathrm{v}})+m\tilde{n}+m^2$	$\tilde{n}=n+r$, $\tilde{n}_h=n_h+n_h^{\mathrm{w}}+n_h^{\mathrm{v}}$, $\tilde{n}_g=n_g+n_g^{\mathrm{w}}+n+n_g^{\mathrm{v}}$
Admissibility	$n^2\tilde{n}_g+nn_g^{\mathrm{x^F}}$	$\tilde{n}_g=n_g+n_g^{\mathrm{w}}+n+n_g^{\mathrm{v}}+m$
Consistency	$\tilde{n}_h(\tilde{n}_h+\tilde{n}_g)^3+n(n+\tilde{n}_g)(n+\tilde{n}_h+\tilde{n}_g)^3+(n^2+m_c)2^n+m_cn\tilde{n}_g+m_c^2$	$\tilde{n}_h=n_h+n_h^{\mathrm{w}}+n_h^{\mathrm{v}}+m+n_h^{\mathrm{x^F}}+n$ $\tilde{n}_g=n_g+n_g^{\mathrm{w}}+n+n_g^{\mathrm{v}}+m+n_g^{\mathrm{x^F}}$
Reduction	$k_c(\tilde{n}_h+\tilde{n}_g)^3+k_cn\tilde{n}_g^2+(n+\varphi_c)^2(\tilde{n}_g-k_c)+k_g(\tilde{n}_g-k_c)(n+\varphi_c)$	$k_c=\tilde{n}_h-\varphi_c$, $k_g=\tilde{n}_g-k_c-\varphi_g$, $\tilde{n}_h=n_h+n_h^{\mathrm{w}}+n_h^{\mathrm{v}}+m+n_h^{\mathrm{x^F}}+n+m_c$, $\tilde{n}_g=n_g+n_g^{\mathrm{w}}+n+n_g^{\mathrm{v}}+m+n_g^{\mathrm{x^F}}+m_c$

To yield punctual estimates $\bar{z}$, and thereby, to approximate the nonlinear models, we make the following choices: CZDC uses the center of the polytope $\mathcal{P}$ associated to Lemma 1, where $\mathcal{P}$ is a box or a parallelotope, whose procedure is $O(1)$; CZFO is run with metric (Rego et al., 2021, $C3$) to minimize the diameter of an interval matrix; CZMV is run with metric (Rego et al., 2021, $C2$) to minimize the diameter of an interval vector. Two performance indexes are computed, namely: (i) the *mean processing time* (T^{CPU}), given by $T^{\mathrm{CPU}} \triangleq \frac{1}{m_s}\frac{1}{k_f}\sum_{j=1}^{m_s}\sum_{k=1}^{k_f} t_{k,j}$, where $k_f \in \mathbb{N}$ is the number of time steps, $m_s \in \mathbb{N}$ is the number of Monte Carlo simulations, and $t_{k,j}$ is the time to execute the kth iteration of a given algorithm in the jth Monte Carlo simulation; and (ii) the *average area ratio of box* ($A^{\Box}$), given by

$$A^{\Box} \triangleq \frac{1}{m_s}\frac{1}{k_f}\sum_{j=1}^{m_s}\sum_{k=1}^{k_f}\prod_{i=1}^{n}\operatorname{diam}\left([x]_{i,k,j}\right),$$

with $\operatorname{diam}([x]) = 2\operatorname{rad}([x])$. The noise terms w_{k-1} and v_k are taken from uniform distributions defined in $\mathcal{W}_{k-1}$ and $\mathcal{V}_k$, while the initial state x_0 belongs to the initial set $\mathcal{X}_0$. The following computer configuration was used: 8 GB RAM 1333 MHz, Windows 10 Pro, and AMD FX-6300 CPU 3.50 GHz. All implementations were executed in MATLAB 9.11 with INTLAB 12 (Rump, 1999), MPT3 (Herceg, Kvasnica, Jones, & Morari, 2013), and Gurobi 10.0.

Since the measurement y_0 is available, all three algorithms execute a first loop with $\mathcal{X}_{k|k-1} = \mathcal{X}_0$, whose goal is to improve the precision of the starting set $\mathcal{X}_0$. Soon after, the state estimators are normally executed. For all examples, CZFO employs order reduction with fixed values φ_c and φ_g at the end of each step, as recommended in Rego et al. (2021).

5.1. Two-state nonlinear process

Consider the nonlinear uncertain system (Alamo et al., 2008)

$$x_k = \begin{bmatrix} -0.7x_{2,k-1} + 0.1x_{2,k-1}^2 + 0.1x_{1,k-1}x_{2,k-1} + 0.1\exp\left(x_{1,k-1}\right) \\ x_{1,k-1} + x_{2,k-1} - 0.1x_{1,k-1}^2 + 0.2x_{1,k-1}x_{2,k-1} \end{bmatrix} + w_{k-1}, \quad (24)$$

$$y_k = x_{1,k} + x_{2,k} + v_k, \quad (25)$$

where $w_{k-1} \in \mathcal{W} = \{0.1\mathrm{I}_2, 0_{2\times 1}\}$ and $v_k \in \mathcal{V} = \{0.2, 0\}$. To simulate this system, we set $x_0 = \begin{bmatrix}1 & 1\end{bmatrix}^{\top} \in \mathcal{X}_0 = \{3 \times \mathrm{I}_2, 0_{2\times 1}\}$, $k_f = 40$, and $m_s = 100$. This example aims at illustrating that CZDC is a promising option to substitute the use of CZFO and CZMV whenever the wrapping and dependency effects imply divergence of estimates, and that CZDC reaches a better precision than the zonotopic filter based on DC programming (ZDC) proposed in Alamo et al. (2008). To reduce order of CZs, we set $\varphi_c = 3$ and $\varphi_g = 8$. This latter value is also used to reduce order of zonotopes in ZDC with Method 4 of Yang and Scott (2018). To improve both the computational efficiency and the precision of the minimum-volume zonotopes computed in ZDC, we employ de Paula et al. (2022, VM3) and Bravo et al. (2006a, Definition 8). Motivated by Alamo et al. (2008), we propose the DC function $x_k = f^{\mathrm{a}} - f^{\mathrm{b}} + w_{k-1}$ such that

$$f^{\mathrm{a}} = \begin{bmatrix} x_{k-1}^{\top}A_1x_{k-1} \\ x_{k-1}^{\top}A_2x_{k-1} \end{bmatrix} + \begin{bmatrix} 0.1\exp\left(x_{1,k-1}\right) \\ x_{1,k-1} + x_{2,k-1} \end{bmatrix} = \begin{bmatrix} 0.1x_{1,k-1}^2 + 0.1x_{1,k-1}x_{2,k-1} + 0.1x_{2,k-1}^2 + 0.1\exp\left(x_{1,k-1}\right) \\ 0.1x_{2,k-1}^2 + x_{1,k-1} + x_{2,k-1} \end{bmatrix},$$

$$f^{\mathrm{b}} = \begin{bmatrix} x_{k-1}^{\top}B_1x_{k-1} \\ x_{k-1}^{\top}B_2x_{k-1} \end{bmatrix} + \begin{bmatrix} 0.7x_{2,k-1} \\ 0 \end{bmatrix} = \begin{bmatrix} 0.1x_{1,k-1}^2 + 0.7x_{2,k-1} \\ 0.1x_{1,k-1}^2 + 0.1x_{2,k-1}^2 - 0.2x_{1,k-1}x_{2,k-1} \end{bmatrix},$$

with A_1, A_2, B_1, and B_2 being positive semidefinite matrices (not necessarily symmetric). Then, there exist different choices of matrices to ensure that f^{a} and f^{b} are convex. Although Hessian matrices could be here chosen as candidate, we present the following choices whose eigenvalues are nonnegative:

$$A_1 = \begin{bmatrix} 0.1 & 0.1 \\ 0 & 0.1 \end{bmatrix}, \quad A_2 = \begin{bmatrix} 0 & 0 \\ 0 & 0.1 \end{bmatrix},$$

$$B_1 = \begin{bmatrix} 0.1 & 0 \\ 0 & 0 \end{bmatrix}, \quad B_2 = \begin{bmatrix} 0.1 & -0.2 \\ 0 & 0.1 \end{bmatrix}.$$

Since DC functions were directly defined, Proposition 4 was not employed, and thereby, the polytope $\mathcal{P}_{k-1}$ associated to Theorem 1 is a parallelotope (given by Proposition 3) that contains the CZ $\mathcal{Z}_{k-1} = \mathcal{X}_{k-1}$.

In Fig. 1(a), we point out that both CZFO and CZMV diverge due to the direct usage of interval arithmetic. In this case, both wrapping and dependency effects are present and lead to large forecasts. Therefore, the application of measurements is not enough to correct the enlargement of CZs over iterations, justifying why those algorithms diverge. Although the direct usage of interval arithmetic was used to experiment CZFO and CZMV in Rego et al. (2021), it is not enough to reach convergence in this case study.

Differently, both ZDC and CZDC achieve convergent solutions because DC programming involves evaluation of elementary functions rather than inclusion functions. In Fig. 1(b) and (c), one-dimensional intervals are sketched to illustrate that those algorithms provide guaranteed solutions. As shown in Table 2, CZDC provides a significantly better precision than ZDC at the cost of a larger total T^{CPU}.

5.2. Attitude estimation

Now, we show the application of CZDC to a more challenging and technological example, containing multiplicative process

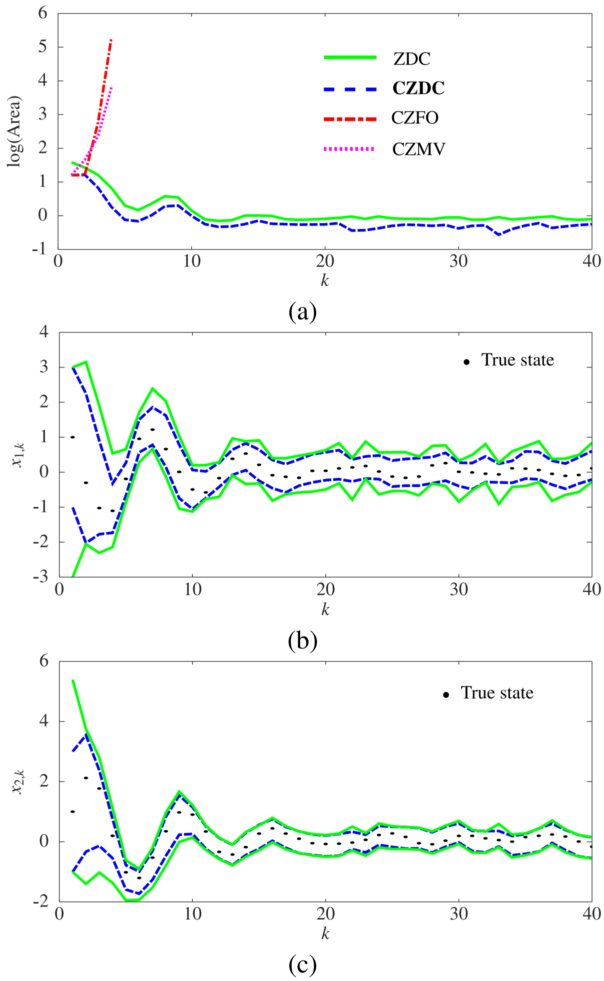

Fig. 1. State estimation for the first case study (Section 5.1). Graph (a) depicts the time evolution of the area of boxes computed by ZDC, CZDC, CZFO, and CZMV. In (b) and (c), true states are involved by interval hulls of CZs computed by ZDC and CZDC.

noise, nonlinear measurements, and state equality constraints. The considered system concerns the attitude estimation of a flying robot. By employing quaternion representation, the attitude is expressed as $x_k \in \mathbb{R}^4$ such that $\|x_k\|_2^2 = 1$. These states evolve at discrete time according to Rego et al. (2021), Teixeira et al. (2009)

$$x_k = \left(\cos\left(p\left(\check{u}_{k-1}\right)\right) \mathrm{I}_4 - \frac{T_s}{2}\frac{\sin\left(p\left(\check{u}_{k-1}\right)\right)}{p\left(\check{u}_{k-1}\right)} \Omega\left(\check{u}_{k-1}\right)\right) x_{k-1}, \tag{26}$$

where $T_s = 0.2$ s is the sampling time, $p\left(\check{u}_k\right) = \frac{T_s}{2}\left\|\check{u}_k\right\|_2$, $\Omega\left(\check{u}_k\right) = \begin{bmatrix} 0 & \check{u}_{3,k} & -\check{u}_{2,k} & \check{u}_{1,k} \\ -\check{u}_{3,k} & 0 & \check{u}_{1,k} & \check{u}_{2,k} \\ \check{u}_{2,k} & -\check{u}_{1,k} & 0 & \check{u}_{3,k} \\ -\check{u}_{1,k} & -\check{u}_{2,k} & -\check{u}_{3,k} & 0 \end{bmatrix}$, and $\check{u}_k = \begin{bmatrix} 0.3\sin\left((2\pi/12)\,kT_s\right) \\ 0.3\sin\left((2\pi/12)\,kT_s - 6\right) \\ 0.3\sin\left((2\pi/12)\,kT_s - 12\right) \end{bmatrix}$ is the physical input that drives the actual system. For state-estimation purposes, we assume that $\check{u}_k$ is acquired by gyroscopes. Then, $\check{u}_k$ is corrupted by an additive noise $w_k \in \mathcal{W} = \left\{3 \times 10^{-3}\mathrm{I}_3, 0_{3\times 1}\right\}$, whose result is the known signal $u_k = \check{u}_k + w_k$. The measurement is given by

$$y_k = \begin{bmatrix} C\left(x_k\right) r^{[1]} \\ C\left(x_k\right) r^{[2]} \end{bmatrix} + v_k, \tag{27}$$

Table 2
Results of T^{CPU} and $A^{\square}$ for the first example (SubSection 5.1). The percentage reduction of $A^{\square}$ for CZDC in comparison with ZDC is shown between parenthesis. The suffixes -F, -D and -R for T^{CPU} denote the elapsed time during, respectively, the forecast, data-assimilation and reduction steps, while -T the total time.

Indexes	ZDC	CZDC
T^{CPU}-F	**1.07** s	1.34 s
T^{CPU}-D	19.7 ms	**0.100** ms
T^{CPU}-R	**0.100** ms	5.90 ms
T^{CPU}-T	**1.09** s	1.35 s
$A^{\square}$	2.16	**1.33** (↓38.4%)

where $r^{[1]} = \begin{bmatrix} 1 & 0 & 0 \end{bmatrix}^\top$, $r^{[2]} = \begin{bmatrix} 0 & 1 & 0 \end{bmatrix}^\top$,

$$C\left(x_k\right) = \begin{bmatrix} x_{1,k}^2 - x_{2,k}^2 - x_{3,k}^2 + x_{4,k}^2 & 2\left(x_{1,k}x_{2,k} + x_{3,k}x_{4,k}\right) & 2\left(x_{1,k}x_{3,k} - x_{2,k}x_{4,k}\right) \\ 2\left(x_{1,k}x_{2,k} - x_{3,k}x_{4,k}\right) & -x_{1,k}^2 + x_{2,k}^2 - x_{3,k}^2 + x_{4,k}^2 & 2\left(x_{1,k}x_{4,k} + x_{2,k}x_{3,k}\right) \\ 2\left(x_{1,k}x_{3,k} + x_{2,k}x_{4,k}\right) & 2\left(-x_{1,k}x_{4,k} + x_{2,k}x_{3,k}\right) & -x_{1,k}^2 - x_{2,k}^2 + x_{3,k}^2 + x_{4,k}^2 \end{bmatrix}$$

is a rotation matrix, and $v_k \in \mathcal{V} = \{0.15\mathrm{I}_6, 0_{6\times 1}\}$.

To simulate the system, we consider the uncorrupted signal $\check{u}_k$, initial state $x_0 = \begin{bmatrix} 0 & 1 & 0 & 0 \end{bmatrix}^\top \in \mathcal{X}_0 = \left\{0.18\mathrm{I}_4, \begin{bmatrix} 0.1 & 0.9 & 0.1 & 0.1 \end{bmatrix}^\top\right\}$, realizations of uniform noise defined in $\mathcal{V}$ for v_k, $k_f = 200$, and $m_s = 10$. To estimate states, we consider the corrupted signal u_k, fixed values $\varphi_c = 10$ and $\varphi_g = 30$, the invariant $g\left(x_k\right) = x_k^\top x_k - 1$, and the feasible set $\mathcal{X}^{\mathrm{F}} = \{\mathrm{I}_4, 0_{4\times 1}\}$. Since $\check{u}_k$ is unknown, the algorithms replace $\check{u}_k$ by $(u_k - w_k)$. Due to the nonlinearity of $x_k = f\left(x_{k-1}, u_{k-1}, w_{k-1}\right)$ in (26), we define the DC function $f = f^{\mathrm{a}} - f^{\mathrm{b}}$ such that $f_i^{\mathrm{a}} = f_i + f_i^{\mathrm{b}}$ and $f_i^{\mathrm{b}} = \frac{\tilde{\lambda}_i}{2} z_{k-1}^\top z_{k-1}$, with $z_{k-1} = \begin{bmatrix} x_{k-1}^\top & w_{k-1}^\top \end{bmatrix}^\top$, $i = 1, \ldots, 4$, and with $\tilde{\lambda}_i$ being given by Proposition 4 over each time step. In this case, the polytope $\mathcal{P}_{k-1}$ related to Theorem 1 is a box (given by Proposition 1) that contains the CZ $\mathcal{Z}_{k-1} = \mathcal{X}_{k-1} \times \mathcal{W}_{k-1}$. By exploiting the quadratic nature of both $y_k = h\left(x_k\right) + v_k$ in (27) and $g\left(x_k\right) = 0$, we propose the DC functions $y_k = h^{\mathrm{a}} - h^{\mathrm{b}} + v_k$ and $g = g^{\mathrm{a}} - g^{\mathrm{b}}$ such that

$$h^{\mathrm{a}} = \begin{bmatrix} x_k^\top A_1 x_k \\ x_k^\top A_2 x_k \\ x_k^\top A_3 x_k \\ x_k^\top A_4 x_k \\ x_k^\top A_5 x_k \\ x_k^\top A_6 x_k \end{bmatrix} = \begin{bmatrix} x_{1,k}^2 + x_{4,k}^2 \\ x_{1,k}x_{2,k} - x_{3,k}x_{4,k} \\ x_{1,k}x_{3,k} + x_{2,k}x_{4,k} \\ x_{1,k}x_{2,k} + x_{3,k}x_{4,k} \\ x_{2,k}^2 + x_{4,k}^2 \\ x_{2,k}x_{3,k} - x_{1,k}x_{4,k} \end{bmatrix}, \quad g^{\mathrm{a}} = g,$$

$$h^{\mathrm{b}} = \begin{bmatrix} x_k^\top B_1 x_k \\ x_k^\top B_2 x_k \\ x_k^\top B_3 x_k \\ x_k^\top B_4 x_k \\ x_k^\top B_5 x_k \\ x_k^\top B_6 x_k \end{bmatrix} = \begin{bmatrix} x_{2,k}^2 + x_{3,k}^2 \\ -x_{1,k}x_{2,k} + x_{3,k}x_{4,k} \\ -x_{1,k}x_{3,k} - x_{2,k}x_{4,k} \\ -x_{1,k}x_{2,k} - x_{3,k}x_{4,k} \\ x_{1,k}^2 + x_{3,k}^2 \\ x_{1,k}x_{4,k} - x_{2,k}x_{3,k} \end{bmatrix}, \quad g^{\mathrm{b}} = 0,$$

where

$$A_1 = \begin{bmatrix} 1 & 0 & 0 & 0 \\ 0 & 0 & 0 & 0 \\ 0 & 0 & 0 & 0 \\ 0 & 0 & 0 & 1 \end{bmatrix}, \quad A_2 = \begin{bmatrix} 0 & 1 & 0 & 0 \\ 0 & 0 & 0 & 0 \\ 0 & 0 & 0 & -1 \\ 0 & 0 & 0 & 0 \end{bmatrix},$$

$$A_3 = \begin{bmatrix} 0 & 0 & 1 & 0 \\ 0 & 0 & 0 & 1 \\ 0 & 0 & 0 & 0 \\ 0 & 0 & 0 & 0 \end{bmatrix},$$

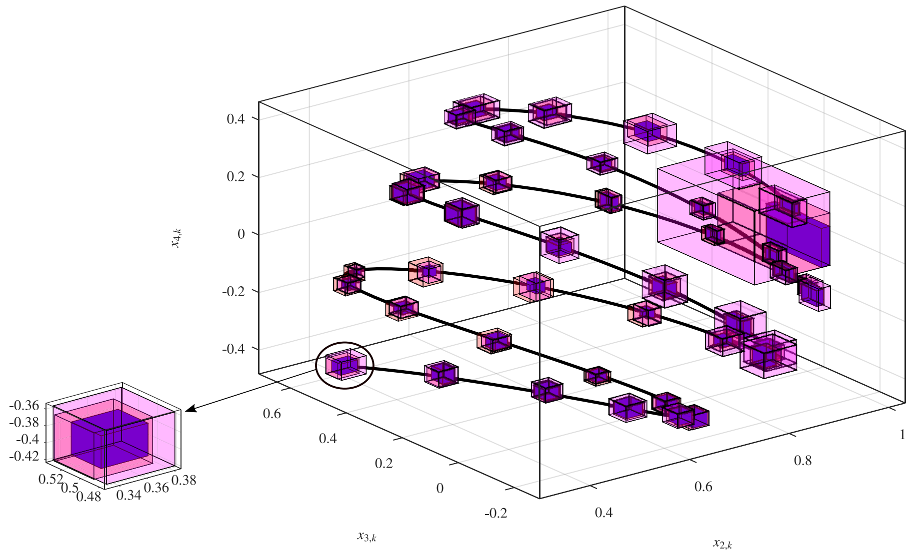

Fig. 2. 3D projection with respect to $x_{1,k} = 0$ of the interval hulls of CZs, computed by CZDC (blue color), CZFO (red color), and CZMV (magenta color), for the second case study (Section 5.2). The true states are sketched in black solid line. (For interpretation of the references to color in this figure legend, the reader is referred to the web version of this article.)

$$A_4 = \begin{bmatrix} 0 & 1 & 0 & 0 \\ 0 & 0 & 0 & 0 \\ 0 & 0 & 0 & 1 \\ 0 & 0 & 0 & 0 \end{bmatrix}, \quad A_5 = \begin{bmatrix} 0 & 0 & 0 & 0 \\ 0 & 1 & 0 & 0 \\ 0 & 0 & 0 & 0 \\ 0 & 0 & 0 & 1 \end{bmatrix},$$

$$A_6 = \begin{bmatrix} 0 & 0 & 0 & -1 \\ 0 & 0 & 1 & 0 \\ 0 & 0 & 0 & 0 \\ 0 & 0 & 0 & 0 \end{bmatrix},$$

$$B_1 = \begin{bmatrix} 0 & 0 & 0 & 0 \\ 0 & 1 & 0 & 0 \\ 0 & 0 & 1 & 0 \\ 0 & 0 & 0 & 0 \end{bmatrix}, \quad B_2 = \begin{bmatrix} 0 & -1 & 0 & 0 \\ 0 & 0 & 0 & 0 \\ 0 & 0 & 0 & 1 \\ 0 & 0 & 0 & 0 \end{bmatrix},$$

$$B_3 = \begin{bmatrix} 0 & 0 & -1 & 0 \\ 0 & 0 & 0 & -1 \\ 0 & 0 & 0 & 0 \\ 0 & 0 & 0 & 0 \end{bmatrix},$$

$$B_4 = \begin{bmatrix} 0 & -1 & 0 & 0 \\ 0 & 0 & 0 & 0 \\ 0 & 0 & 0 & -1 \\ 0 & 0 & 0 & 0 \end{bmatrix}, \quad B_5 = \begin{bmatrix} 1 & 0 & 0 & 0 \\ 0 & 0 & 0 & 0 \\ 0 & 0 & 1 & 0 \\ 0 & 0 & 0 & 0 \end{bmatrix},$$

$$B_6 = \begin{bmatrix} 0 & 0 & 0 & 1 \\ 0 & 0 & -1 & 0 \\ 0 & 0 & 0 & 0 \\ 0 & 0 & 0 & 0 \end{bmatrix}.$$

Remark 7. Hessian matrices are not here candidate to replace the prior non-symmetric matrices. To achieve that, new functions h^{a} and h^{b} must be defined, but this procedure may enlarge the current eigenvalues, yielding more conservative DC approximations.

Having in mind the choice of matrices here adopted, the polytopes $\mathcal{P}_k$ and $\check{\mathcal{P}}_k$, in Theorem 2 and Corollary 1, are parallelotopes (given by Proposition 3) that contain the CZs $\mathcal{Z}_k = \mathcal{X}_{k|k-1}$ and $\check{\mathcal{Z}}_k = \check{\mathcal{X}}_k$, respectively. We employ parallelotopes instead of boxes because the DC components are fixed, and thereby, $\mathcal{P}_k$ and $\check{\mathcal{P}}_k$ may reach better precision.

Fig. 2 depicts a separate simulation with the CZDC, CZFO and CZMV algorithms. Boxes were sketched rather than CZs for computational simplicity. According to the figure, CZDC generates CZs with the smallest associated interval hulls. Moreover, a faster reduction of uncertainty is expected with CZDC during the initialization effect. Table 3 corroborates the improvement of precision caused by CZDC in comparison with both CZMV and CZFO. Since CZFO is, in general, more costly than CZMV (Rego et al., 2021, Table 1), it demands a larger total T^{CPU} as shown in Table 3. Differently, CZDC can enhance the precision of CZMV using much less computational resource, and this advantage is related to both tight linearization remainder (Lemma 1) and low-dimension CZs (Remark 6). However, the quantity of operations involved with CZDC may be larger than the CZMV one, justifying the difference of T^{CPU}.

In order to verify if the precision of CZDC would be enlarged with respect to Table 3 (reduction of $A^{\square}$), we also tested if convexifying each row of f or $-f$, for each time step, would be better (Remark 2), selecting the strategy with the smallest lower bound of eigenvalue. However, the tests pointed out that convexifying f always yielded the best solutions.

During the state estimation, CZMV and CZFO diverged for some simulations, whose results were discarded and not included in the computation of $A^{\square}$. In this case, the enlargement of CZs was increasing, but fixed by the admissibility step, resulting in the own feasible set $\mathcal{X}^{\mathrm{F}}$. In principle, the prior results could be improved with the increase of φ_c and φ_g. However, the generator reduction can imply conservatism for some directions due to the wrapping effect. This effect is influenced by the evolution of CZs, which is different for each Monte Carlo simulation since the noise realizations are present in u_k and y_k, affecting then the intersections.

For completeness, the ZDC algorithm was also tested with five steps. The box constraints, represented by $\mathcal{X}^{\mathrm{F}}$, were enforced using the steps 2–11 of de Paula et al. (2022, Algorithm 3). For all simulations, ZDC diverged and demanded a total T^{CPU} around 110 s because of the volume minimization. Differently, CZDC reached convergence and demanded a much smaller T^{CPU} as shown by Table 3.

6. Conclusions

This paper proposed a new set-membership filter for discrete-time nonlinear uncertain systems with state constraints, called CZDC. A DC programming approach was used to provide a new nonlinear approximation for CZs. Thus, CZDC established an alternative estimation basis with respect to the state-of-the-art algorithms, called CZMV and CZFO (Rego et al., 2021). We showed

Table 3
Results of T^{CPU} and $A^{\square}$ for the second example (SubSection 5.2). The percentage reduction of $A^{\square}$ for CZDC and CZFO in comparison with CZMV is shown between parenthesis. The suffixes -F, -D, -A, -C and -R for T^{CPU} denote the elapsed time during, respectively, the forecast, data-assimilation, admissibility, consistency and reduction steps, while -T the total time.

Indexes	CZDC	CZFO	CZMV
T^{CPU}-F	3.70 s	12.9 s	**1.26** s
T^{CPU}-D	0.265 s	6.48 s	**0.162** s
T^{CPU}-A	**38.7** μs	57.7 μs	55.7 μs
T^{CPU}-C	0.278 s	**0.164** s	0.302 s
T^{CPU}-R	**0.0207** s	20.6 s	0.473 s
T^{CPU}-T	4.26 s	40.1 s	**2.20** s
$A^{\square}(\times 10^{-4})$	**0.0244** (↓97.4%)	0.189 (↓79.9%)	0.939

that the performance of these two algorithms can be significantly deteriorated due to the wrapping and dependency effects, with CZDC being a good option to mitigate divergence and conservatism issues. Over two numerical examples, we discussed advantages of CZDC over CZMV and CZFO. These three algorithms can readily enforce linear inequality constraints on the state vector by using CZs. However, the nonlinear case requires investigation and will be intended in the future. Other challenge is the proof of convergence for CZDC. Currently, the interval bounds returned by Lemma 1 are only guaranteed, being then necessary a technique that additionally delimits the extreme values.

Acknowledgments

This work was partially supported by the Brazilian agencies CNPq, under grants 465755/2014-3 (INCT project), 315695/2020-0, and 306564/2020-3; FAPESP, under grant 2014/50851-0; CAPES, under the grants 001 and 88887.136349/2017-00; FAPEMIG, under grant APQ-03090-17 and by the Italian Ministry for Research in the framework of the 2017 Program for Research Projects of National Interest (PRIN) (Grant No. 2017YKXYXJ).

References

Adjiman, C. S., & Floudas, C. A. (1996). Rigorous convex underestimators for general twice-differentiable problems. *Journal of Global Optimization*, *9*(1), 23–40.
Alamo, T., Bravo, J. M., & Camacho, E. F. (2005). Guaranteed state estimation by zonotopes. *Automatica*, *41*(6), 1035–1043.
Alamo, T., Bravo, J. M., Redondo, M., & Camacho, E. F. (2008). A set-membership state estimation algorithm based on DC programming. *Automatica*, *44*(1), 216–224.
Althoff, M., Stursberg, O., & Buss, M. (2008). Reachability analysis of nonlinear systems with uncertain parameters using conservative linearization. In *2008 47th IEEE conference on decision and control* (pp. 4042–4048).
Bravo, J. M., Alamo, T., & Camacho, E. F. (2006a). Bounded error identification of systems with time-varying parameters. *IEEE Transactions on Automatic Control*, *51*(7), 1144–1150.
Bravo, J. M., Alamo, T., & Camacho, E. F. (2006b). Robust MPC of constrained discrete-time nonlinear systems based on approximated reachable sets. *Automatica*, *42*(10), 1745–1751.
Bravo, J. M., Alamo, T., Redondo, M. J., & Camacho, E. F. (2008). An algorithm for bounded-error identification of nonlinear systems based on DC functions. *Automatica*, *44*(2), 437–444.
Chisci, L., Garulli, A., & Zappa, G. (1996). Recursive state bounding by parallelotopes. *Automatica*, *32*(7), 1049–1055.
Combastel, C. (2005). A state bounding observer for uncertain non-linear continuous-time systems based on zonotopes. In *2005 IEEE 44th conference on decision and control* (pp. 7228–7234).
de Paula, A. A., Raffo, G. V., & Teixeira, B. O. S. (2022). Zonotopic filtering for uncertain nonlinear systems: Fundamentals, implementation aspects, and extensions [applications of control]. *IEEE Control Systems*, *42*(1), 19–51.
Di Marco, M., Garulli, A., Giannitrapani, A., & Vicino, A. (2004). A set theoretic approach to dynamic robot localization and mapping. *Autonomous Robots*, *16*(1), 23–47.
Grocholsky, B., Stump, E., & Kumar, V. (2006). An extensive representation for range-only SLAM. In *International symposium on experimental robotics, 2006, Rio de Janeiro* (pp. 1–10).
Hast, D., Findeisen, R., & Streif, S. (2015). Detection and isolation of parametric faults in hydraulic pumps using a set-based approach and quantitative–qualitative fault specifications. *Control Engineering Practice*, *40*, 61–70.
Herceg, M., Kvasnica, M., Jones, C., & Morari, M. (2013). Multi-parametric toolbox 3.0. In *Proc. of the European Control Conference* (pp. 502–510). Zürich, Switzerland: http://control.ee.ethz.ch/~mpt.
Ifqir, S., Puig, V., Ichalal, D., Ait-Oufroukh, N., & Mammar, S. (2020). Zonotopic set-membership estimation for switched systems based on wi-radius minimization: Vehicle application. *IFAC-PapersOnLine*, *53*(2), 7446–7451.
Li, S., Stouraitis, T., Gienger, M., Vijayakumar, S., & Shah, J. A. (2021). Set-based state estimation with probabilistic consistency guarantee under epistemic uncertainty. arXiv preprint arXiv:2110.09584.
Mesbah, A. (2016). Stochastic model predictive control: An overview and perspectives for future research. *IEEE Control Systems Magazine*, *36*(6), 30–44.
Pourasghar, M., Puig, V., & Ocampo-Martinez, C. (2019). Interval observer versus set-membership approaches for fault detection in uncertain systems using zonotopes. *International Journal of Robust and Nonlinear Control*, *29*(10), 2819–2843.
Rego, B. S., Locatelli, D., Raimondo, D. M., & Raffo, G. V. Joint state and parameter estimation based on constrained zonotopes. *Automatica*, accepted, http://arxiv.org/abs/2204.09740.
Rego, B. S., Raffo, G. V., Scott, J. K., & Raimondo, D. M. (2020). Guaranteed methods based on constrained zonotopes for set-valued state estimation of nonlinear discrete-time systems. *Automatica*, *111*, Article 108614.
Rego, B. S., Scott, J. K., Raimondo, D. M., & Raffo, G. V. (2021). Set-valued state estimation of nonlinear discrete-time systems with nonlinear invariants based on constrained zonotopes. *Automatica*, *129*, Article 109638.
Rump, S. (1999). INTLAB - interval laboratory. In T. Csendes (Ed.), *Developments in Reliable Computing* (pp. 77–104). Dordrecht: Kluwer Academic Publishers, http://www.ti3.tuhh.de/rump/.
Scott, J. K., Raimondo, D. M., Marseglia, G. R., & Braatz, R. D. (2016). Constrained zonotopes: A new tool for set-based estimation and fault detection. *Automatica*, *69*, 126–136.
Tabatabaeipour, S. M., Odgaard, P. F., Bak, T., & Stoustrup, J. (2012). Fault detection of wind turbines with uncertain parameters: A set-membership approach. *Energies*, *5*(7), 2424–2448.
Tao, P. D., & An, L. T. H. (1997). Convex analysis approach to DC programming: theory, algorithms and applications. *Acta Mathematica Vietnamica*, *22*(1), 289–355.
Teixeira, B. O. S., Chandrasekar, J., Tôrres, L. A., Aguirre, L. A., & Bernstein, D. S. (2009). State estimation for linear and non-linear equality-constrained systems. *International Journal of Control*, *82*(5), 918–936.
Wang, Y., Blesa, J., & Puig, V. (2017). Robust periodic economic predictive control based on interval arithmetic for water distribution networks. *IFAC-PapersOnLine*, *50*(1), 5202–5207.
Xu, F., Puig, V., Ocampo-Martinez, C., Olaru, S., & Stoican, F. (2015). Set-theoretic methods in robust detection and isolation of sensor faults. *International Journal of Systems Science*, *46*(13), 2317–2334.
Yang, X., & Scott, J. K. (2018). A comparison of zonotope order reduction techniques. *Automatica*, *95*, 378–384.

Alesi A. de Paula received the B.S. degree in electrical engineering from the Federal Center for Technological Education of Minas Gerais, Brazil, in 2016, with first-class honors. He received the M.Sc. and Doctor degrees in electrical engineering from the Federal University of Minas Gerais, Brazil, in 2018 and 2022, respectively. His main research interests are in state estimation and mixed-uncertainty representation.
https://orcid.org/0000-0002-8043-1956

Davide M. Raimondo earned his Ph.D. in Electronics, Computer Science, and Electrical Engineering from the University of Pavia, Italy, in 2009. Following this, he embarked on a Postdoctoral Fellowship at the Automatic Control Laboratory, ETH Zürich, Switzerland, from 2009 to 2010. He subsequently served as an Assistant Professor at the University of Pavia from 2010 to 2015, and later as an Associate Professor from 2015 to 2021. In December 2021, he was appointed as a Full Professor at the same institution, a position he held until September 2023. Since October 2023, Dr. Raimondo has assumed the role of Full Professor at the University of Trieste. Over the course of his career, Dr. Raimondo has also held visiting positions at several institutions including MIT, Cambridge, MA, USA; the University of Seville, Seville, Spain; TU Wien, Vienna, Austria; and the University of Konstanz, Konstanz, Germany. Dr. Raimondo is the author or co-author of more than

100 papers published in refereed journals, books, and conference proceedings. His primary research interests encompass a wide array of topics, including battery management systems, set-based estimation, fault diagnosis, fault-tolerant control, model predictive control, and optimization. Dr. Raimondo, along with his co-authors, received the prestigious 2014–2016 Automatica Paper Prize Award in 2017, and the SAFEPROCESS Best Student Paper Award in 2022. Dr. Raimondo is also a Subject Editor for Automatica and IEEE Transactions on Control Systems Technology. Since 2022, he has held the title of IEEE senior member.

https://orcid.org/0000-0003-4249-7935

Guilherme V. Raffo received the B.Sc. degree in automation and control engineering from the Pontifical Catholic University of Rio Grande do Sul, Brazil, in 2002, the Specialist degree in industrial automation from the Federal University of Rio Grande do Sul, Brazil, in 2003, the M.Sc. degree in electrical engineering from the Federal University of Santa Catarina, Brazil, in 2005, and the M.Sc. degree in automation, robotics and telematic and the Ph.D. degree from the University of Seville, Spain, in 2007 and 2011, respectively. From 2011 to 2012, he was a Postdoctoral Fellow with the Federal University of Santa Catarina. He is currently an Associate Professor with the Federal University of Minas Gerais, Brazil. He is also co-head of the MACRO Research Group — Mechatronics, Control, and Robotics since March 2014. He is the author or coauthor of more than 145 publications, including journal articles, book chapters, and conference proceedings. His current research interests include robust non-linear optimal control theory, predictive control and set-membership estimation, seeking to apply these techniques to tracking problems with avoidance features, conversion between flight modes, cargo transportation using UAVs, aerial manipulation, and coordination of multi-UAVs.

https://orcid.org/0000-0002-1835-8380

Bruno O.S. Teixeira received the B.S. in control and automation engineering (first-class honors) in 2004 and the Doctor degree in electrical engineering in 2008, both from the Federal University of Minas Gerais, Brazil, where he is currently an associate professor in the Department of Electronic Engineering. He was a visiting scholar in the Aerospace Engineering Department at the University of Michigan in 2006–2007. His main interests are in state estimation and system identification, including applications on aeronautics, robotics and oil industry.

https://orcid.org/0000-0001-7608-0391